

## Lightning Activity in a Hail-Producing Storm Observed with Phased-Array Radar

C. EMERSIC\*

*Cooperative Institute for Mesoscale Convective Systems, University of Oklahoma, and NOAA/National Severe Storms Laboratory, Norman, Oklahoma*

P. L. HEINSELMAN AND D. R. MACGORMAN

*NOAA/National Severe Storms Laboratory, Norman, Oklahoma*

E. C. BRUNING

*Cooperative Institute for Climate and Satellites, Earth System Science Interdisciplinary Center, University of Maryland, College Park, College Park, Maryland*

(Manuscript received 30 July 2010, in final form 9 October 2010)

### ABSTRACT

This study examined lightning activity relative to the rapidly evolving kinematics of a hail-producing storm on 15 August 2006. Data were provided by the National Weather Radar Testbed Phased-Array Radar, the Oklahoma Lightning Mapping Array, and the National Lightning Detection Network.

This analysis is the first to compare the electrical characteristics of a hail-producing storm with the reflectivity and radial velocity structure at temporal resolutions of less than 1 min. Total flash rates increased to approximately  $220 \text{ min}^{-1}$  as the storm's updraft first intensified, leveled off during its first mature stage, and then decreased for 2–3 min despite the simultaneous development of another updraft surge. This reduction in flash rate occurred as wet hail formed in the new updraft and was likely related to the wet growth; wet growth is not conducive to hydrometeor charging and probably contributed to the formation of a “lightning hole” without a mesocyclone. Total flash rates subsequently increased to approximately  $450 \text{ min}^{-1}$  as storm volume and inferred graupel volume increased, and then decreased as the storm dissipated.

The vertical charge structure in the storm initially formed a positive tripole (midlevel negative charge between upper and lower positive charges). The charge structure in the second updraft surge consisted of a negative charge above a deep midlevel positive charge, a reversal consistent with the effects of large liquid water contents on hydrometeor charge polarity in laboratory experiments.

Prior to the second updraft surge, the storm produced two cloud-to-ground flashes, both lowering the usual negative charge to ground. Shortly before hail likely reached ground, the storm produced four cloud-to-ground flashes, all lowering the positive charge. Episodes of high singlet VHF sources were observed at approximately 13–15 km during the initial formation and later intensification of the storm's updraft.

### 1. Introduction

This study examines the evolution of lightning activity in an Oklahoma summertime storm at 2220–2258 UTC

---

\* Current affiliation: Centre for Atmospheric Science, University of Manchester, Manchester, United Kingdom.

---

*Corresponding author address:* Dr. Pamela Heinselman, National Severe Storms Laboratory, 120 David L. Boren Blvd., Norman, OK 73072.  
E-mail: pam.heinselman@noaa.gov

on 15 August 2006 that produced hail aloft but did not have supercell characteristics. It was chosen for analysis because of the datasets available from the National Weather Radar Testbed Phased-Array Radar (NWRT PAR), which provided sector volume scans in 26 s, and from the Oklahoma Lightning Mapping Array (LMA), which mapped lightning inside the cloud in three spatial dimensions with  $80\text{-}\mu\text{s}$  temporal resolution and 40–50-m spatial resolution (Thomas et al. 2004). Data from the National Lightning Detection Network (NLDN) and National Weather Service soundings also were utilized. This combined dataset allowed us to examine the

relationships of lightning to evolving storm kinematics with much higher temporal resolution than has been possible previously.

A previous study by Heinselman et al. (2008) examined the detailed evolution of kinematic features of the storm revealed by NWRT PAR data and described the environmental conditions that produced the storm; this paper will focus on the lightning that the storm produced. Of particular relevance to this paper is Heinselman et al.'s observation of a strong three-body scatter spike (TBSS; e.g., Zrnić 1987) and associated 65–75-dBZ reflectivity values, which indicated the presence of wet hail within the storm. The eventual descent of these signatures toward the ground suggests that this was a hail-storm (see section 3b), even though no confirming reports of hail reaching ground are available from the rural area where the storm occurred. Hence, the storm is termed a hail-producing storm. Even though polarimetric radar data are unavailable for this storm, it is possible to examine lightning characteristics associated with the presence of hail inferred from the TBSS and high-reflectivity signatures in the NWRT PAR data.

One might expect lightning behavior to be related to the presence of moderate-to-large hail because the electrification of storms is thought to be influenced strongly by ice microphysics. Laboratory studies have shown that, independent of the ambient electric field, rebounding collisions between ice crystals and riming graupel particles transfer enough charge between the hydrometeors to account for the electric field magnitudes observed in thunderstorms (e.g., Takahashi 1978; Jayaratne et al. 1983; Pereyra et al. 2000; Saunders et al. 2006). Many observational and simulation studies of storms have also supported the hypothesis that graupel and ice crystals are the species that play the most vital role in the electrification of storms and the occurrence of lightning (e.g., Dye et al. 1988; Ziegler et al. 1991; Brangi et al. 1997; Black and Hallett 1999; Bruning et al. 2007). The microphysical process responsible for this charge exchange is still somewhat uncertain, but laboratory studies indicate that mass is transferred during ice particle collisions, and the particle whose surface is growing fastest from vapor diffusion at the instant of collision charges positively on particle separation (the relative diffusional growth rate mechanism) (Baker et al. 1987; Dash et al. 2001; Mitzeva et al. 2005; Emersic and Saunders 2010).

Subsequent differential sedimentation of the graupel and smaller ice particles separates the two charge polarities to produce regions of increasing net charge, which in turn produce electric fields that can increase to the point of causing lightning [see the discussion in section 3.4 of MacGorman and Rust (1998)]. Such electric

breakdown is expected to originate between oppositely charged regions [as discussed, e.g., by MacGorman et al. (1981), Mansell et al. (2002); Coleman et al. (2003)], consistent with the limited observations of lightning initiations near the boundary between a region of graupel and surrounding regions of smaller ice particles (e.g., Lund et al. 2009).

In most thunderstorms, midlevel graupel at the  $-15^{\circ}$  to  $-20^{\circ}\text{C}$  isotherm charges negatively, and ice crystals positively. Because the lighter ice crystals tend to be lofted to higher regions, thunderclouds usually contain an upper positive charge region on small ice particles, with a midlevel negative charge region sourced by the heavier falling graupel. Frequently, a lower region of positive charge is observed that is usually attributed to graupel charging positively at higher temperatures (Jayaratne and Saunders 1984). Occasionally, however, storms are observed with vertical charge structure opposite to normal (Rust and MacGorman 2002; Yijun et al. 2002). Although the cause of such a charge structure is still uncertain, it may be related to a storm's microphysics; the most recent published laboratory studies have shown that the local environment in which cloud and precipitation ice particles interact strongly influences the resulting polarity of the graupel charge (Saunders et al. 2004, 2006; Emersic and Saunders 2010).

Like many severe storms analyzed in the scientific literature (e.g., Rust et al. 1981; MacGorman et al. 1989; Carey and Rutledge 1998; Schultz et al. 2009), the hail-producing storm on 15 August 2006 produced hundreds of flashes per minute, and the largest, most rapid increase in flash rates occurred near the time large hail formed. In this paper we use the high temporal resolution data provided by the NWRT PAR to analyze, more closely than has been possible with conventional radar antennas, how flash rates and other lightning characteristics relate to the evolution of storm structure and hail growth. Our goal is to improve the current understanding of how storm processes influence lightning production, in part to determine better which storm characteristics can be diagnosed from lightning mapping observations for use by forecasters.

## 2. Instrumentation

### *a. National Weather Radar Testbed Phased-Array Radar*

The NWRT PAR is a 9.4-cm wavelength, electronically steered radar located in Norman, Oklahoma (Zrnić et al. 2007). Because this instrument was originally developed for military purposes, the beam is vertically polarized.

Given that a raindrop becomes flatter with increasing diameter, the magnitude of the reflectivity can be somewhat diminished compared to the reflectivity observed with a horizontally polarized beam.

This single-faced phased-array system scans a  $90^\circ$  sector while stationary; the particular  $90^\circ$  sector is selected by mechanical steering. Stationary scanning eliminates the beam smearing produced by mechanically scanning radars. Unlike conventional radars, the beamwidth varies azimuthally: perpendicular to the antenna face (i.e., along the bore site) the beamwidth is  $1.5^\circ$ ; away from the bore site the beamwidth increases gradually to  $2.1^\circ$ . The range resolution is 240 m and the sensitivity is 5.9 dBZ at 50 km.

The 15 August 2006 storm studied in this paper is one of the first scanned by the NWRT PAR. Because data quality algorithms had not yet been employed, the data contained some ground clutter, second-trip echo, and sidelobe contamination. Although these data quality issues can be problematic, Heinselman et al. (2008) noted that in this case they did not have a significant adverse impact. Both reflectivity and radial velocity data were analyzed by Heinselman et al. (2008); only reflectivity data are shown in this paper.

The primary goal for data collection was to capture the evolution of a hail-producing storm at higher spatial and temporal resolutions than were available with the Weather Surveillance Radar-1988 Doppler (WSR-88D). Data were collected with a scanning strategy that contained 31 elevation angles ranging from  $0.5^\circ$  to  $41^\circ$ . The volume scan time was decreased to 26 s by employing a pulse repetition time (PRT) of  $831 \mu\text{s}$ , with 12 pulses per dwell at each elevation angle. Although reducing the number of pulses per dwell diminished the accuracy of the radial velocity estimates compared to traditional WSR-88D scans ( $\pm 1 \text{ m s}^{-1}$ ), the errors were within  $\pm 2 \text{ m s}^{-1}$ . The associated Nyquist velocity, approximately  $29 \text{ m s}^{-1}$ , also reduced the potential for velocity aliasing.

### b. Lightning Mapping Array

The design of the Lightning Mapping Array (LMA) is described by Rison et al. (1999). At each of six or more stations having 13–23-km baselines between them, the Oklahoma LMA (OK-LMA) measures the arrival time of impulsive VHF radiation produced in the channel 3 VHF television band (60–66 MHz) by lightning discharge processes, to locate the sources of VHF radiation in three spatial dimensions and time (Rison et al. 1999; MacGorman et al. 2008).

The accuracy of the mapped source locations in the region of the hail-producing storm we analyzed is expected to be within 10 m in the horizontal dimension, 30 m

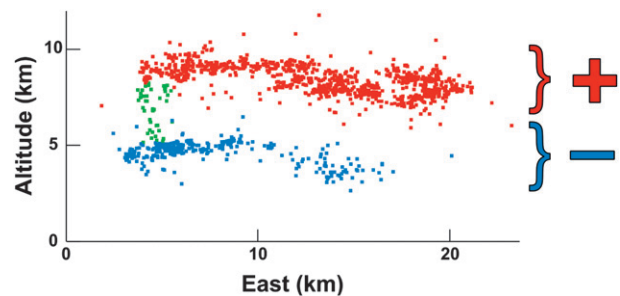


FIG. 1. An example of using VHF sources mapped by the LMA to infer the storm charge structure involved in a flash. Negative breakdown within a positive charge (red dots) leads to many more VHF sources being detected relative to positive breakdown in a negative charge (blue dots). The green dots indicate the initial breakdown of a negative leader, in this case, propagating upward into a positive charge.

in the vertical dimension, and 40 ns in time (Thomas et al. 2004). VHF sources detected by fewer than seven stations, or with a reduced  $\chi^2$  greater than 2, were not used in this study because their locations were considered less reliable. The system mapped at most one VHF source per  $80\text{-}\mu\text{s}$  window, giving a maximum rate of approximately  $12\,000 \text{ s}^{-1}$ . The LMA has been used in many studies to examine the three-dimensional and temporal structures of lightning during a storm's lifetime (e.g., Krehbiel et al. 2000; Lang et al. 2004; MacGorman et al. 2005; Bruning et al. 2007; Rioussset et al. 2007; Kuhlman et al. 2009).

The polarity and extent of charge through which lightning propagated were inferred from the sequence and density of points mapped by the LMA, as described by Wiens et al. (2005), Rust et al. (2005), and MacGorman et al. (2008). Briefly, breakdown processes at the negative end of the channel (which propagates mostly in regions of positive storm charge) tend to produce stronger signals in the VHF band than those produced by the positive end (which propagates mostly in negative charge regions) and so are almost always the first processes to be detected in a flash. Because their signals tend to be stronger, negative breakdown processes produce many more mapped points. The initial direction of channel development, the relative density of points, and the sequence of later channel development all are used to infer the charge polarity through which each channel propagates. Additional information about this process is given by Shao and Krehbiel (1996), Rison et al. (1999), and MacGorman et al. (2008), and comparisons of the charge inferred from lightning with charge regions inferred from electric field soundings are provided by Coleman et al. (2003), Rust et al. (2005), and MacGorman et al. (2008). An example of the storm charge inferred from a lightning flash is shown in Fig. 1.

### c. Other datasets

NLDN data (Biagi et al. 2007) were used to identify which flashes struck ground, along with the polarity of charge lowered to the ground and their ground strike locations. NLDN detections were compared to LMA data to help discriminate between cloud and ground flashes with low peak currents (roughly, less than 15 kA). Smaller inferred peak currents tend to be associated with cloud flashes, although some valid ground flashes do have small peak currents. Thirty-six negative (lowering negative charge) and four positive flashes (lowering positive charge) were detected in the data presented here. All negative ground strikes after 2215 UTC were less than 15 kA and were treated as false detections except where the LMA showed evidence of a negative leader propagating toward ground at the correct time and location during the overall flash duration.

This study also made use of the 0000 UTC atmospheric sounding from the National Weather Service Forecast Office in Norman, Oklahoma (OUN), on 16 August 2006. This sounding was chosen because of its proximity in space (<50 km) and time (1–2 h after) to the storm.

## 3. Evolution of lightning and inferred storm charge structure

### a. Period 1: First flash rate increase (2220–2234 UTC)

The lightning activity throughout most of the storm's lifetime is summarized in Fig. 2. Figure 3 shows a sequence of vertical cross sections of reflectivity spanning most of what is defined here as period 1, which persists from the storm's initial radar echo through the first peak in lightning flash rates. The storm's initial reflectivity core was first detected at 2220 UTC, approximately 1 km west of an existing storm, as shown in the first panel of Fig. 3. The relatively infrequent lightning flashes shown between 2210 and 2220 UTC in Figs. 2 and 4 were initiated by previous storms, including the older storm shown in Fig. 3. One valid negative ground flash (−19.7 kA at 2214:36 UTC) was detected by the NLDN during this time, with the other lightning flashes likely being cloud flashes (i.e., flashes that did not reach ground).

The older storm shown in Fig. 3 [at radial distance 19–23 km in panels (a)–(e); 2220:41–2225:53 UTC] reached its maximum vertical extent and maximum mid-level reflectivity at 2220–2222 UTC; flash rates increased between 2218 and 2222 UTC as this storm intensified. The charge structure inferred from LMA data revealed that this storm had a classic tripole charge structure, with a midlevel negative charge sandwiched between upper and lower positive charges (Fig. 5). The lower positive charge was between 2 and 5 km MSL, the midlevel negative

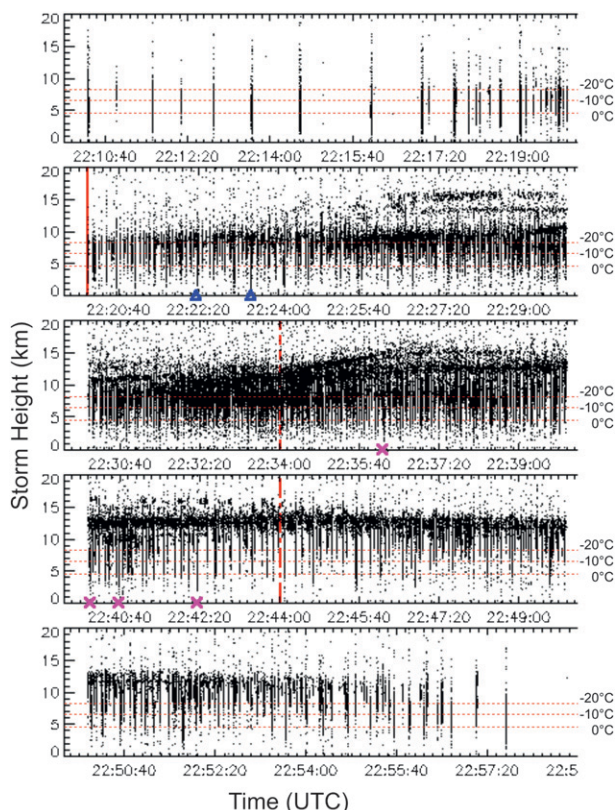


FIG. 2. The altitude and time of VHF sources mapped by the LMA. Individual black vertical line–like features denote individual flashes; during active periods, many such lines merge into general black regions. Symbols on the horizontal axis represent suspected ground lightning strike times of a given polarity detected by NLDN: blue triangles represent negative ground strikes; magenta crosses represent positive ground strikes. The solid red vertical line denotes the start of period 1 of the storm, the dashed line represents the start of period 2, and the dotted–dashed line represents the start of period 3.

charge was between 6 and 9 km MSL, and the upper positive charge was above 10 km MSL. The environmental freezing level determined by the 0000 UTC sounding on 16 August 2006 was at an altitude of approximately 4.5 km MSL, with the  $-10^{\circ}$  and  $-20^{\circ}\text{C}$  isotherms located at 6.5 and 8.3 km MSL, respectively.

After 2222 UTC, the older storm appeared to be dissipating, as its reflectivity  $>35$  dBZ began decreasing in maximum height and descending to lower altitudes, where it expanded horizontally. However, the new storm to its west grew rapidly during this period and merged with the dissipating storm. Heinselman et al. (2008) noted radial divergence aloft and an increasing area and magnitude of convergence at low levels during this period, indicative of a strong updraft. In the 8 min following the first detection of reflectivity in this new storm at 2220 UTC, the lightning flash rate increased to approximately  $220 \text{ min}^{-1}$

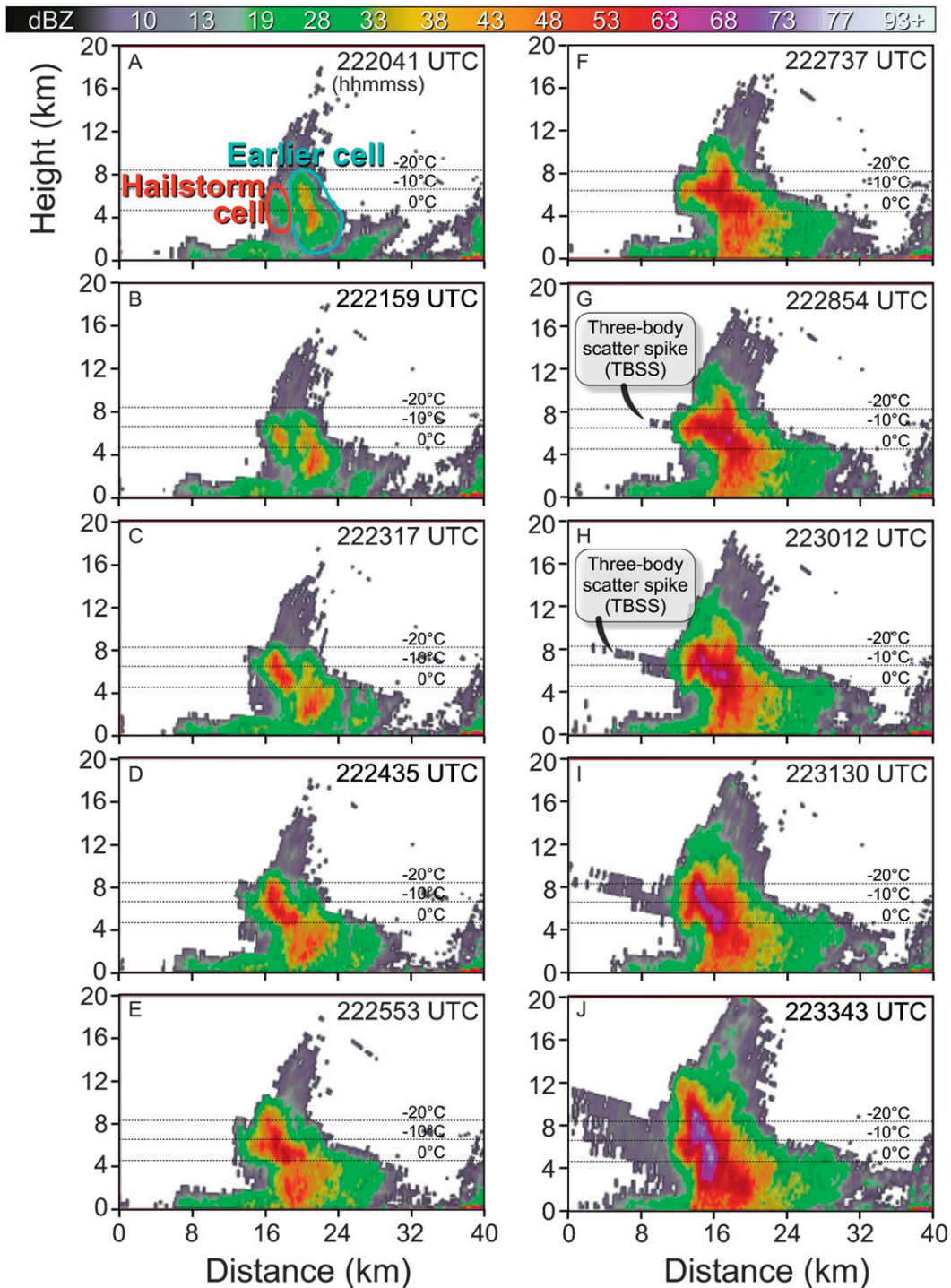


FIG. 3. First ~13 min of radar reflectivity data of the hail-producing storm on 15 Aug 2006 constituting period 1 of the storm; for brevity, one or two volume scans were skipped between each panel shown. Each panel shows a vertical cross section of reflectivity (dBZ) taken along a 40-km-long line along the azimuth through the storm's early reflectivity core. Increasing horizontal axis values correspond to decreasing distance from the NWRT PAR (0 is approximately 50 km from the NWRT PAR).

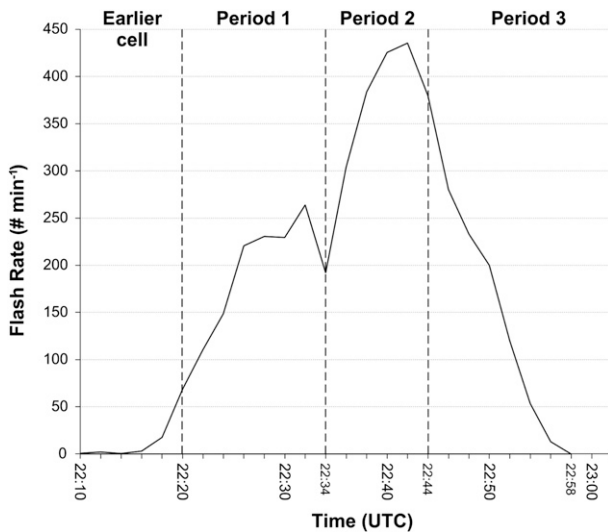


FIG. 4. Time series plot of flash rates determined from OK-LMA data of the three storm life cycle periods analyzed for this study.

(Fig. 4), as the storm's reflectivity increased in magnitude, altitude, and vertical extent (Fig. 3). Of the flashes occurring between 2220 and 2234 UTC (Fig. 2), none were positive ground flashes, and two were negative ground flashes with peak currents of  $-7.8$  and  $-9.2$  kA indicated by the NLDN. The LMA data for both of these ground flashes suggested negative leaders propagating toward the surface, consistent with identifying the flashes as ground flashes. Such propagation was absent for 12 other NLDN detections, some of which had slightly larger peak currents than the two ground strikes we considered to be valid.

Because of the new storm's close proximity to the older storm, it was difficult to tell when the new storm began initiating lightning, but lightning began involving the new storm at approximately the time that its 30-dBZ reflectivity appeared, shortly after 2220 UTC. The 30-dBZ reflectivity first appeared between 6 and 7 km MSL, at roughly  $-10^{\circ}\text{C}$ , well below the  $-20^{\circ}\text{C}$  isotherm at 8.3 km MSL. Having lightning activity begin when a region of 30-dBZ reflectivity has reached only the  $-10^{\circ}\text{C}$  isotherm is a lesser threshold than has been observed in many studies, although it is not unprecedented (section 7.18 of MacGorman and Rust 1998). Furthermore, lightning initiated elsewhere may propagate into a storm before it is electrified enough to initiate lightning itself (Lund et al. 2009). The location of the storm's initial reflectivity echoes above the freezing level means that ice was likely present, consistent with ice being important to cloud charging.

Analysis of LMA data suggests that lightning flashes that could be identified as beginning within the new storm often traveled into charge that remained in the older

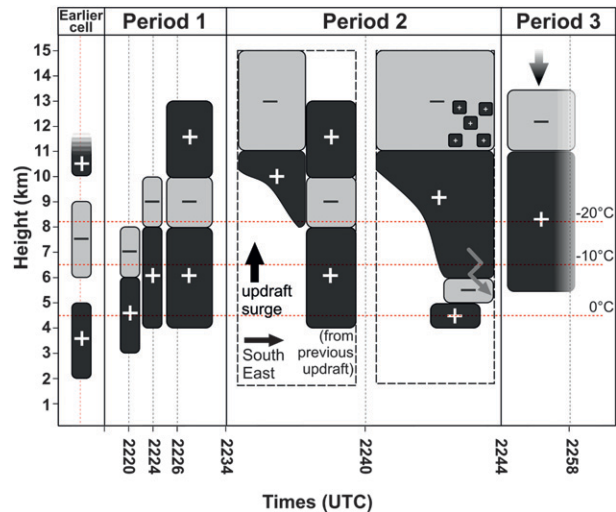


FIG. 5. Summary of the vertical charge structure of the developing storm inferred from OK-LMA data during each analyzed period of its lifetime. Box width is not related to the relative spatial extent of the charge regions; however, height is representative.

dissipating storm. The LMA analysis suggests further that the new storm's charge structure initially formed a negative dipole, with a midlevel negative charge above a lower positive charge. The lower positive charge was present from the onset of lightning in the new storm (Fig. 5), initially at an altitude of 3–6 km but increasing to 4–8 km by 2224 UTC as radar echoes increased to higher altitudes. Similarly, the height of the midlevel negative charge was initially 6–8 km and increased to 8–10 km by 2224 UTC. The upper positive charge shown in Fig. 5 at an altitude of 10–13 km did not become apparent in LMA lightning data until after 2226 UTC, when 20-dBZ reflectivity began to extend above 10 km (Fig. 3).

Between 2226 and 2230 UTC, an upper band of unusual VHF radiation sources became visible in the LMA data at a height of 13–15 km (Fig. 2). This band occurred shortly after flash rates increased to more than  $200 \text{ min}^{-1}$  (Fig. 4), after the altitude of the 35-dBZ reflectivity grew rapidly to 10 km MSL (2223:17–2225:53 UTC in Fig. 3), and while an adjoining bounded weak-echo region (BWER) was developing (2225:53–2228:54 UTC in Fig. 3). Heinselman et al. (2008) reported development of an area of low- to middle-altitude convergence in the radial velocity below the BWER during this same period. Together these observations indicate that the storm updraft was intensifying and deepening. The upper band of VHF radiation consisted of continual single radiation sources occurring at a rate of several per second, rather than consisting of the episodic flashes of 10 or more VHF sources typically found at lower altitudes. The upper band of VHF radiation existed for only 4 min, ending at

2230 UTC, when the tallest 35-dBZ turret had begun dissipating. No radar reflectivities were clearly detected in the altitude band of the upper VHF sources, but 20-dBZ reflectivities extended up to at least 12 km and it is possible that still weaker storm reflectivities extended higher but were obscured by the sidelobe contamination (Doviak and Zrnić 1993) apparent above the storm during this period. Because the upper discharges disappeared as the tallest 35-dBZ turret began dissipating, it appears that their disappearance was caused by the cessation of a strong updraft pulse.

Flash rates stopped their rapid increase and leveled off between 2226 and 2234 UTC (Figs. 2 and 4). As noted above, a BWER formed (at radial distance 13–16 km in Fig. 3) adjacent to the previous storm updraft during this period, indicative of a new updraft surge (Foote and Frank 1983). The region of >35-dBZ reflectivity above the BWER grew rapidly upward, reaching an altitude of 12 km by the end of the period at 2234 UTC. At 2229 UTC and an altitude of 6–7 km, reflectivity >60 dBZ and the TBSS began appearing—a signature of wet hail having formed (e.g., Zrnić 1987). The maximum value of reflectivity and the depth both of highest reflectivity and of the TBSS increased in a region slanting downward and eastward from just above the BWER to the precipitation core below the older updraft.

From studies relating increasing flash rates to increasing updraft mass flux and to increasing graupel mass (e.g., Carey and Rutledge 1998, 2000; Wiens et al. 2005; Kuhlman et al. 2006), one might expect that the flash rate would increase rapidly from 2226 to 2234 UTC during the development of the BWER and the observed increase in the height of moderate to large reflectivities associated with a second updraft pulse. We suggest two possible reasons why there was only a small increase in flash rates followed by a decrease to just under  $200 \text{ min}^{-1}$  during 2234–2236 UTC (Fig. 4), when the storm was still growing rapidly upward, as will be shown in section 3b.

The first possibility is that the development of a downdraft in the vicinity of the first updraft surge coincided with the development of the subsequent updraft surge. The core of reflectivity >45 dBZ in the region of the first surge reached ground at approximately 2226 UTC and began spreading horizontally, until it extended below the first tower of strong reflectivity and the height of the tower began falling. As a result, the increase in flash rate due to storm growth associated with the second surge may have been offset by the decrease in flash rates in the vicinity of the downdraft. The second possible reason is related to the evidence for wet hail growth during this period. The present paradigm for thunderstorm electrification is that it primarily involves field-independent charge exchange during rebounding collisions

of riming graupel and cloud ice in the mixed-phase region (Saunders et al. 2004; Wiens et al. 2005; Saunders et al. 2006; MacGorman et al. 2008; Emersic and Saunders 2010). If graupel is collecting supercooled water droplets fast enough to be in surface wet growth, cloud ice colliding with it will rarely, if ever, rebound. The implication is that those parts of the mixed-phase region having a wet hail signature will produce little, if any, charge exchange between graupel and cloud ice, as observed in laboratory studies (Saunders and Brooks 1992; Pereyra et al. 2000). An additional consequence of increased collection efficiencies of colliding riming particles during wet surface growth conditions, particularly in the presence of large hail, is that the number of electrically significant particles will decrease, to further diminish collision-based charging processes. This interpretation is bolstered by the relative lack of lightning, sometimes called a lightning hole, above the BWER in the region having a wet hail signature (Fig. 6) from 2232 to 2234 UTC. In this case, the lightning hole is not associated with a mesocyclone—contrary to all other examples of such a phenomenon available in the literature to date—but is associated with the wet hail signature. The scenario of graupel wet growth is probably the main exception to the tendency for flash rates to increase with increasing growth of frozen precipitation in the mixed-phase region.

*b. Period 2: Second flash rate increase  
(2234–2244 UTC)*

During period 2 (2234:08–2244:05 UTC; Fig. 8) we can see that the storm grew vertically to its highest altitude. During 2236:44–2238:02 UTC, the 40-dBZ reflectivity reached approximately 14 km and the 20-dBZ reflectivity reached 15 km. After 2238:02 UTC, the 40-dBZ turret subsided to 12 km, while the region of >20-dBZ reflectivity began spreading horizontally to form an anvil at 8–14 km, much of the growth being in the volume having 30–40-dBZ reflectivity. The region of largest reflectivity (>65 dBZ) and the TBSS marking the presence of large, wet hail both descended throughout the period; the TBSS reached ground and disappeared as this period ended.

The last updraft surge discussed previously appeared to change the charge structure of the storm substantially, but initially only within the updraft region. Instead of the original upper-level positive charge over a midlevel negative charge, the new charge structure had an upper-level negative charge (11–15 km) over a deep midlevel positive charge (8–11 km) (Fig. 5). In the region elevated by strong updraft, the lightning involved in this region initially became vertically compressed at a higher altitude (Fig. 2). The midlevel positive charge region extended to lower altitudes to the south and east, while

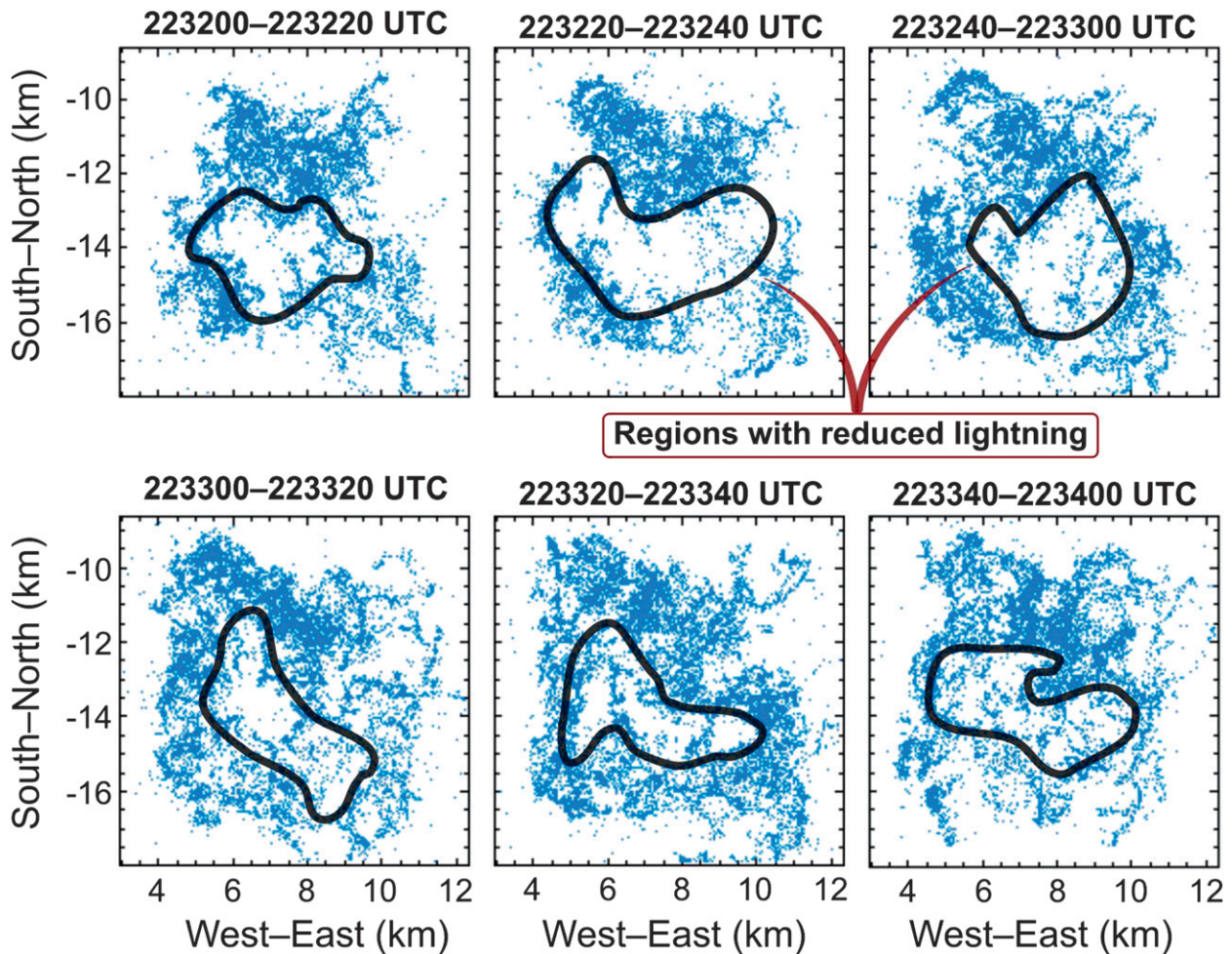


FIG. 6. Plan-view plot of accumulated VHF sources from lightning in 20-s intervals during a 2-min period of the maximum presence of wet hail inferred from the highest radar reflectivity and a three-body scatter spike. An absence of lightning can be seen within the hail region giving rise to a net lightning hole. This is the first instance of a lightning hole associated with an inferred wet hail presence instead of the strong rotating updraft of a mesocyclone.

retaining the same maximum altitude (Fig. 5). In a narrow ( $\sim 3$  km wide) region east of the BWER, outside the main updraft, the original positive tripole structure remained. Combined, the charge regions in the new and old updraft surges produced a horizontal double dipole, with regions of opposite polarity charge horizontally displaced from each other at the same altitude.

By approximately 2240 UTC, the lofted charge structure having a negative charge above a positive charge became prevalent throughout the storm, overwhelming most of the previous region of upper-level positive charge over midlevel negative charge. The only remnants of the previous midlevel negative charge over lower positive charge were much shallower and lower in the storm, with negative charge at 5–6 km and positive charge at 4–5 km. All that was left of the previous upper positive charge region were some pockets of positive charge embedded

within the new upper negative charge region, but south and east of the new updraft region (Fig. 5). An analysis of the lightning channels in the upper storm regions, above the in-cloud structure of ground flashes, indicated that the channels propagated mainly through negative storm charge, suggesting that the anvil that formed around this time became predominantly negatively charged (Fig. 5).

For most of period 2, from 2236 to 2244 UTC, flash rates increased rapidly to their largest value of almost  $450 \text{ min}^{-1}$  at 2242 UTC, more than doubling their previous value at 2234 UTC (Fig. 4). The large increase in flash rates probably was related to the large growth observed in the volume of the storm within 8–14 km MSL, which would be caused, at least in part, by an increase in the updraft mass flux from levels below 8 km. Similar relationships among lightning flash rates with the volume

of graupel mass and updraft mass flux have been noted, for example, by Wiens et al. (2005) and Kuhlman et al. (2006).

This period produced all four of the storm's positive ground strikes and no negative strikes (Fig. 2). The increase in ground flash rates was possibly related to the increasing volume of precipitation at the middle levels of the storm, as found by MacGorman et al. (1989, 2007). The storm's first positive ground strike was reported on the northern side of the hail shaft at 2236:08 UTC. Its low peak current of +15.3 kA and LMA structure more similar to other negative dipole cloud flashes raise questions about the flash's identification by the NLDN as a cloud-to-ground flash. The remaining positive ground flashes identified by the NLDN during this period appear to be correctly identified. Two positive strikes (peak currents of +133.9 and +107.4 kA at 2240:20 and 2240:38 UTC, respectively) arose from positive leaders propagating through part of the small low region of negative charge extending southeast of the storm at 5–6 km MSL (Fig. 5). The final positive ground strike at 2242:17 UTC (peak current +66.6 kA) occurred on the northern side of the storm. A positive leader propagated to the surface away from the flash origin at an altitude of 8 km; positive storm charge was generally inferred south of the flash origin at 5–9 km. The ground strikes during this time came to the ground at the side of the hail shaft (Fig. 7), as observed by Changnon (1992). Lightning similarly avoided a polarimetric signature of wet growth in Bruning et al. (2007).

One final observation during this most electrically active period of the storm's lifetime was the reemergence of an upper band of continual single VHF radiation sources (Fig. 2). The occurrence of this upper band of sources coincided well with the period when the storm had a small overshooting top (Fig. 8). The upper radiation sources occurred continuously for 4 min, until 2240 UTC, and ended when the height of the 40-dBZ reflectivity stopped increasing and began subsiding, and as the 15-dBZ top began leveling out, with the region of the former turret becoming almost indistinguishable from the anvil in reflectivity.

#### c. Period 3: Flash rate decrease (2244–2258 UTC)

During this period, lightning flash rates diminished from their peak value to the end of the lightning activity (Fig. 4). The sequence of vertical cross sections in Fig. 9 shows that the maximum reflectivity and the maximum height of most reflectivity values decreased steadily during this dissipation period. The upper band of isolated VHF sources had disappeared by the start of this period, and the altitude of larger VHF source densities also decreased (Fig. 2). From the start of this period until

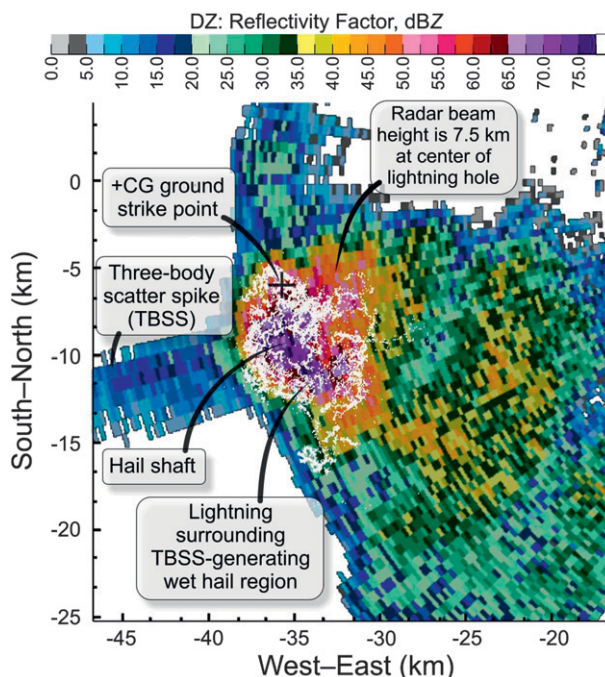


FIG. 7. Radar and LMA lightning data overlay showing lightning surrounding the hail shaft, where hail is inferred to be in wet growth due to the presence of the three-body scatter spike. Only lightning in the vicinity of the hail shaft is shown for clarity in viewing storm structure. The LMA data are taken from a 20-s period approximately during the time of the bottom-right panel in Fig. 6 and correlate closely with the time of the radar image. The distances shown are from the radar origin and not from the center of the LMA network. The radar elevation here was 11°, corresponding to an altitude of 7.5 km at the center of the lightning hole.

the lightning ceased, analysis of LMA data indicated that the negative dipole structure from the updraft surge was prevalent, but that charge regions descended by approximately 1 km (Figs. 2 and 5). No confirmed ground flashes occurred during this period.

## 4. Discussion and summary

This study examined lightning activity during 2218–2258 UTC on 15 August 2006 in an Oklahoma storm that produced hail aloft. Rapid scans of reflectivity and radial velocity were acquired by the National Weather Radar Testbed Phased-Array Radar (NWRT PAR) in Norman, Oklahoma. Total lightning activity was mapped in three dimensions by the Oklahoma Lightning Mapping Array (LMA), and cloud-to-ground lightning strikes were located by the National Lightning Detection Network (NLDN) and checked by comparing with LMA data.

The 26-s volume scans provided by the NWRT PAR revealed cycles of storm growth too rapid to be well resolved in the volume scans of WSR-88D and other

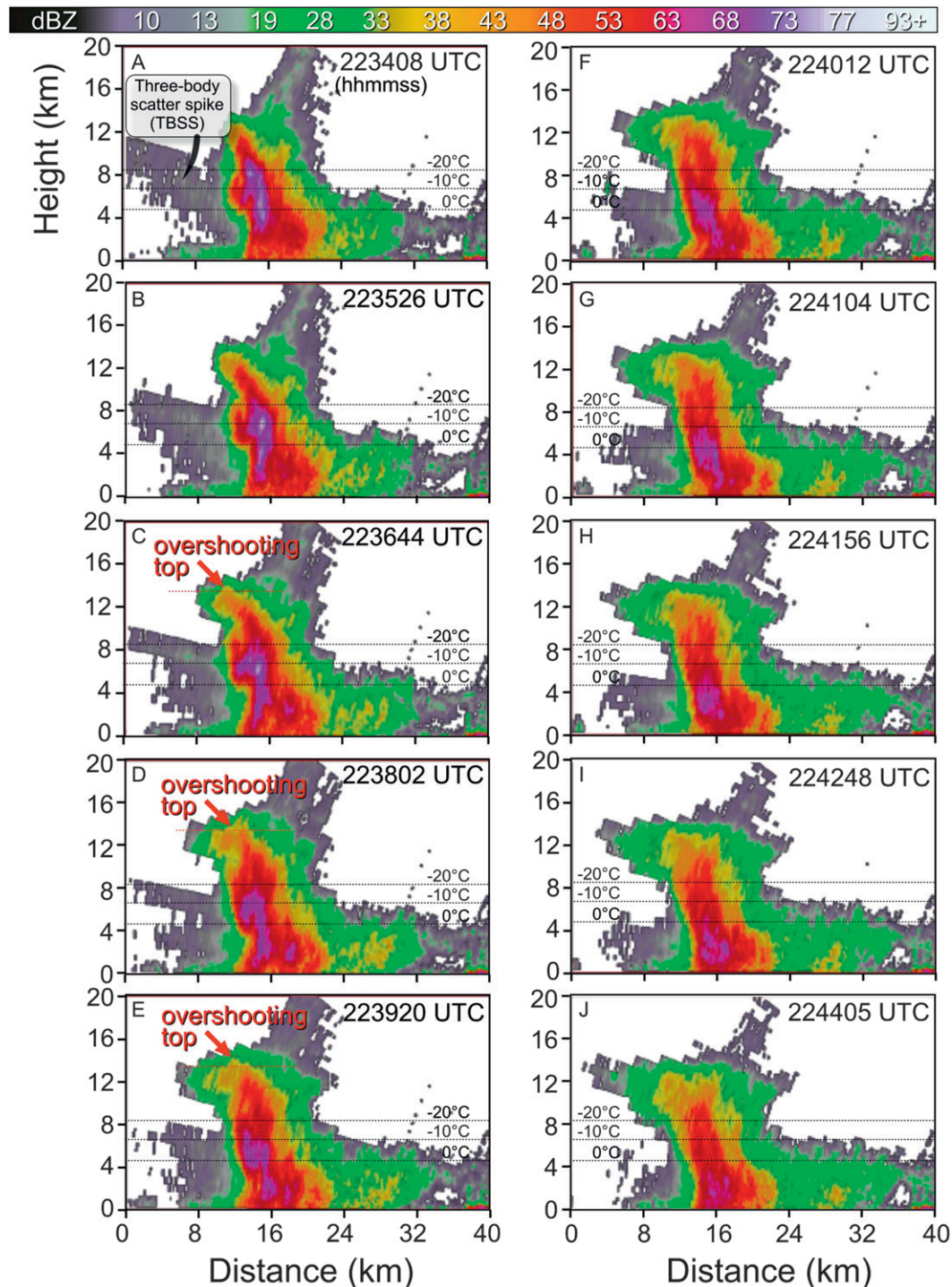


FIG. 8. Analogous to Fig. 3, but showing the radar reflectivity for period 2 of the hail-producing storm on 15 Aug 2006.

conventional radars, which typically require  $\geq 4$  minutes per volume scan. The  $>45$ -dBZ reflectivity cores of the storm that were the focus of our study appeared and grew to their maximum vertical extent in 8–10 min—a period that would be sampled by at most two (and

perhaps only one) complete volume scans of many traditional radars. The NWRT PAR's ability to determine the appearance and maximum vertical extent of a new reflectivity core to within less than 1 min was important for our study examining lightning trends that varied

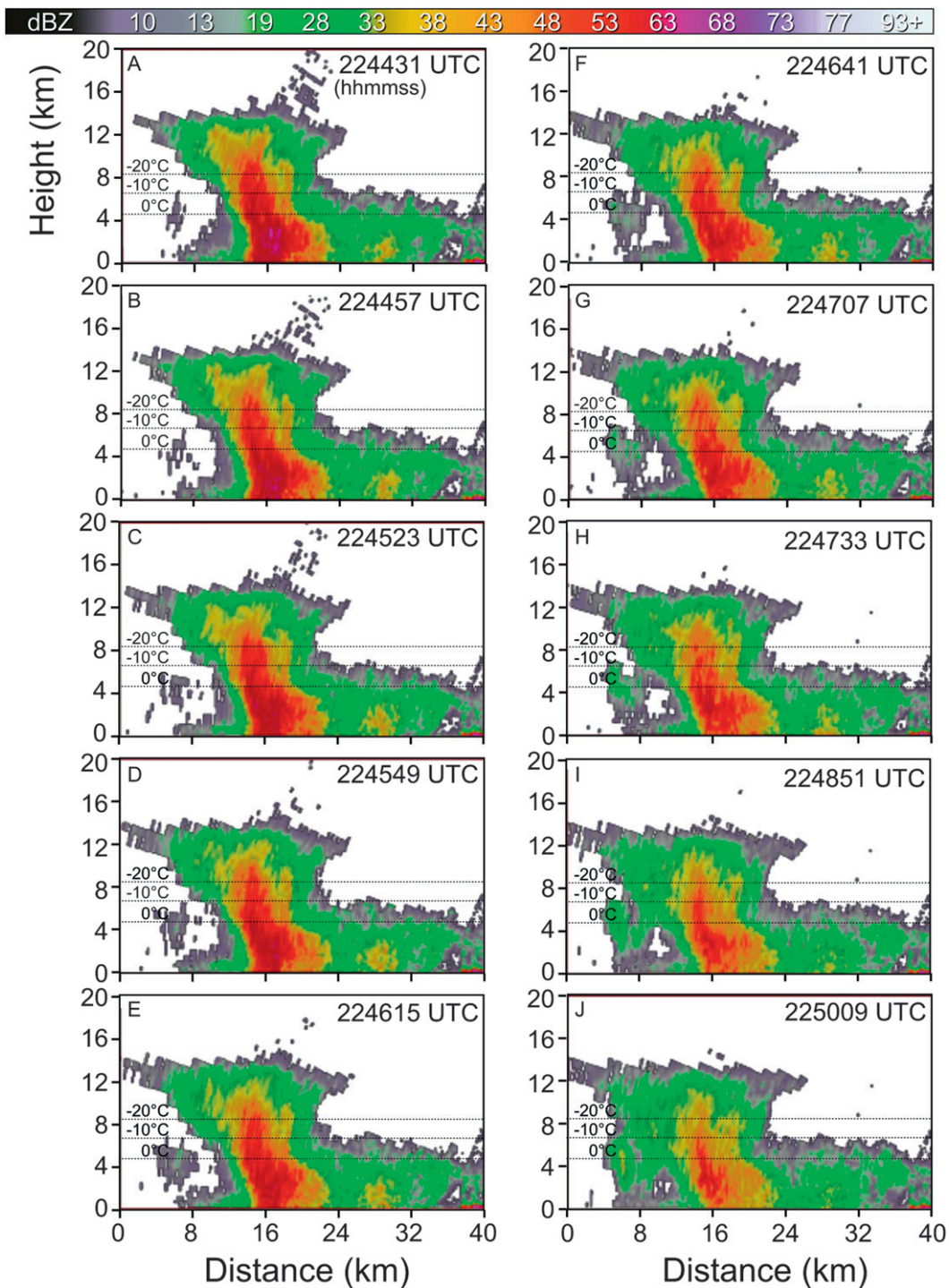


FIG. 9. Analogous to Fig. 3, but showing the radar reflectivity for period 3 of the hail-producing storm on 15 Aug 2006.

markedly over periods of 2–8 min relative to the growth and dissipation of storms. Prominent observed lightning phenomena and their relationship to storm kinematics and microphysics are discussed in the following subsections.

*a. High-altitude bands of VHF radiation*

One aspect of our study for which high temporal resolution NWRTPAR data were important was an analysis of a transient, upper band of VHF radiation consisting

of a fairly steady rate of mostly single isolated VHF sources, which occurred during two episodes. The initial occurrence of this band coincided with the initial strong, vertical growth of the hail-producing storm. The first upper band of isolated VHF radiation sources began when the region of 40-dBZ reflectivity reached a maximum altitude of approximately 10 km, and it ceased as the maximum height of the 40-dBZ reflectivity began decreasing in the storm 3–4 min later. (There was no upper band of VHF radiation for previous storms, which were shallower.) This VHF radiation occurred at an altitude of approximately 13–15 km, above a vertically growing reflectivity echo, and was 1–4 km above the highest region of 30-dBZ reflectivity for the entire period of its occurrence. It appears that the reflectivity at the location of most upper sources was below the minimum detectable level of the NWRT PAR, but it is possible that radar sidelobe contamination obscured some features near storm top in the vicinity of the upper VHF sources for at least part of the period.

The second transient upper band of isolated VHF sources began approximately 6 min later, when the 40-dBZ reflectivity echo of an updraft surge reached its maximum altitude of approximately 13 km, and again ended when the larger reflectivities began decreasing in the upper part of the storm 4 min later. Like the first band, these VHF sources were at an altitude of approximately 15 km, but unlike the first band, the 30-dBZ reflectivity extended up almost to 15 km throughout the period during which the band occurred. Also unlike the first band, which appeared abruptly at 15 km, the second band appeared to be the apex of a rising relative maximum of lightning density [a feature Ushio et al. (2003) called a lightning bubble], which had begun rising 2 min earlier from an altitude of approximately 11 km (Fig. 2). There was also a coincident increase in the maximum height of the larger reflectivities. The high temporal resolution of NWRT PAR allowed us to directly observe this relationship between the high isolated VHF sources and the increasing altitude of the storm.

It is not clear from our data what caused this upper band of continual single radiation sources. The lower threshold for electric field breakdown at upper altitudes of the storm probably was a factor. Taylor et al. (1984), who observed somewhat similar continual, scattered VHF sources in the upper part of a severe storm, suggested that the discharges occurred between the uppermost charge inside the thunderstorm and a screening-layer charge that formed on the cloud boundary [e.g., section 3.5.4 of MacGorman and Rust (1998)]. Regarding our observation of lightning in the overshooting top, it is possible that eddies along the cloud boundary may have folded the screening-layer charge into the cloud interior

to interact with a charge rising in the updraft and thereby to produce electric field magnitudes large enough to cause lightning. Such a possibility is supported by the observations of Blythe et al. (1988) and Stith (1992), who used tracers to show that the upper cloud boundary is entrained into the upper cloud. Polarimetric radar data or in situ measurements may be needed to shed more light on this phenomenon.

#### *b. Cloud-to-ground lightning*

Only 37 ground flashes were reported by the NLDN in the storm analyzed here, and only 6 were confidently verified as ground flashes by comparison with associated LMA data. Of the six likely ground flashes, the first two occurred during the first analyzed period of the storm (see section 3a) and lowered the usual negative charge to ground (negative ground flashes), with low peak currents of  $-7.8$  and  $-9.2$  kA (Fig. 2). All four of the ground flashes that lowered a positive charge (positive ground flashes, with peak currents of  $+15.3$ ,  $+133.9$ ,  $+107.4$ , and  $+66.6$  kA, respectively) occurred during the second analyzed period (see section 3b), when the total flash rate grew to be much greater than the maximum observed during period 1. The first positive ground flash occurred approximately 5 min before the main hail region was inferred from radar data to have reached ground, with the rest occurring as the hail was reaching ground, a pattern of behavior similar to that observed by MacGorman and Burgess (1994). No further ground flashes were detected during the rest of the storm's lifetime.

As in the cases observed by MacGorman et al. (1981, 1983) and Wiens et al. (2005), lightning channels within the hail-producing storm analyzed here, including the in-cloud channels of cloud-to-ground lightning, tended to avoid a region of wet hail indicated by a TBSS and radar reflectivity  $>60$  dBZ. Bruning et al. (2007) made a similar observation of lightning tending to avoid a region of likely surface wet growth of frozen hydrometeors but observed this in a small, nonsevere thunderstorm. Similarly, we observed that lightning tended to strike ground to the side of the hail shaft, not within the hail shaft. This finding is consistent with previous studies: Carey and Rutledge (1998), for example, noted that ground strike points in a severe Colorado hailstorm avoided regions of active hail fall. In a study of Illinois hailstorms, Changnon (1992) found that lightning struck ground to the sides of hail streaks.

Negative ground flashes were initiated between a mid-level region of negative charge and a lower region of positive charge in period 1. Positive ground flashes were initiated as the storm intensified between a new deep midlevel region of positive charge and a transient lower

region of negative charge through which lightning leaders propagated to the ground.

The source of the lower positive charge thought to be necessary for producing most negative ground flashes (e.g., Jacobson and Krider 1976; MacGorman et al. 2001; Mansell et al. 2002) has been a matter of some debate. Marshall and Winn (1982) suggested that the lower positive charge is deposited by lightning. However, an initial lower positive charge was present from lightning onset in the storm we analyzed, as in the storm analyzed by Bruning et al. (2007) and modeled by Mansell et al. (2010). It is known from laboratory experiments that graupel tends to charge positively at higher temperatures (e.g., Takahashi 1978; Saunders and Peck 1998; Saunders et al. 2004; Emersic and Saunders 2010). Thus, the lower positive charge region observed in period 1 of the storm was most likely caused by graupel that had interacted with ice crystals in environments warmer than roughly  $-10^{\circ}\text{C}$ . The development of the upper region of positive charge occurred later in period 1, after the lower two charge regions had already formed, and is consistent with many studies and observations suggesting that lighter ice crystals rising in the updraft were the charge carriers for the uppermost positive charge.

The lower negative charge thought similarly to be necessary to initiate most positive ground flashes (e.g., MacGorman et al. 2001; Mansell et al. 2002) appeared in this case to be the descending remnant of the previous midlevel negative charge region as the storm produced its first downdraft. The positive charge through which positive ground flashes propagated was the deep midlevel region of positive charge elevated in the updraft surge during period 2 and had no low-level charge directly below it. The greater height of the lowest charge in the updraft surge is consistent with the elevating effects of strong updrafts on charge height, as suggested by MacGorman et al. (1989, 2005, 2007). Several studies (e.g., Wiens et al. 2005; Williams et al. 2005; Carey and Buffalo 2007) have suggested that strong broad updrafts are more conducive to the formation of midlevel positive charge, because laboratory studies (e.g., Saunders et al. 2004, 2006; Emersic and Saunders 2010) have found that graupel tends to gain positive charge when interacting with ice particles in regions of relatively large liquid water content, across a broad range of environmental temperature. MacGorman et al. (2008) noted that this process would produce a negative dipole charge structure, but that the midlevel positive charge could interact with a lower negative charge in adjoining storms to produce positive ground flashes, as observed in this case. The complex patterns of temporal and spatial evolution of the charge regions throughout the storm's lifetime is consistent with suggestions that the charge

structure of a storm is not a product just of the charge generated locally, but also is a result of the history and transport of charge carriers in the cloud, as noted by MacGorman et al. (2008), Bruning (2008), and Bruning et al. (2010).

Many thousands of flashes occurred in this storm, but less than 1% of the flashes were cloud-to-ground flashes. Several other studies (e.g., Rust et al. 1981; MacGorman et al. 1989; Carey and Rutledge 1998; Shafer et al. 2000) have similarly noted that cloud-to-ground flashes compose only a small percentage of all flashes in many severe storms, particularly in storms whose vertical polarity of charge structure is opposite to the usual polarity (i.e., negative charge is uppermost in the main tripole or dipole involved in lightning, instead of the usual positive charge) or which produce ground flashes lowering a positive charge to the ground, instead of the usual negative charge.

MacGorman et al. (1989, 2005, 2007) suggested in other cases that the small fraction of flashes striking ground was caused by a severe storm's very strong updraft. The strong updraft lifted the formation and growth of the frozen hydrometeor charge carriers to higher altitudes than is usual in storms, and caused the resulting charge to remain relatively high for substantial periods. Because cloud-to-ground flashes require not only a degree of electrification strong enough to initiate flashes, but a configuration of cloud charge that would cause a channel to propagate to ground, they argued that the higher altitude and close proximity of oppositely charged regions resulting from strong updrafts in severe storms were more favorable than usual for cloud flashes and less favorable than usual for the formation of a cloud-to-ground channel. MacGorman et al. (1989, 2005, 2007) also noted that cloud-to-ground lightning production may be inhibited in severe storms by the time required to form and transport downward the precipitation carrying the low-level charge region, which is needed to initiate lightning from the oppositely charged midlevel charge region. These arguments are consistent with our findings of substantial cloud lightning during a time when an elevated and horizontal dipole charge structure was present (Fig. 5), and with the increased lightning ground flash occurrence when transient lower charge regions were present as discussed above.

### *c. Total lightning relative to kinematics and microphysics*

Our observations at early analysis times indicate that the extension of lightning to a new storm coincided with the appearance of a new region of 20–30-dBZ radar reflectivity above the freezing level—a relationship suggesting that ice presence was important to the storm's

electrification processes. Our observations are consistent in that respect with numerous recent observational and laboratory studies, as discussed in the introduction. Lightning activity began, however, when the height of the 30-dBZ reflectivity was below the  $-20^{\circ}\text{C}$  isotherm, the threshold reported by several previous studies of winter thunderstorms in Japan (Michimoto 1991; Kitagawa 1992; Maekawa et al. 1992; Michimoto 1993; Kitagawa and Michimoto 1994). It also is below the altitude range postulated by MacGorman et al. (1989) and Ziegler and MacGorman (1994), who suggested that the interacting ice hydrometeors needed to be located 7–9 km above mean sea level (between  $-25^{\circ}$  and  $-40^{\circ}\text{C}$ ) before lightning would occur.

This discrepancy may not reflect a physical difference among storms, however, because most of the above-referenced studies examined the beginning of lightning production by a storm, while our analysis examined the initial time lightning involved an updraft pulse that formed within a few kilometers of an older updraft pulse that was already producing lightning. The timing we observed suggests that electrification began by the time the 30-dBZ radar reflectivity reached the  $-20^{\circ}\text{C}$  isotherm of the ambient environment (likely corresponding to a somewhat warmer level in the updraft region) but may not yet have occurred at a large enough rate to initiate lightning in an isolated storm when it first reached that altitude. Lund et al. (2009) showed that a cell embedded in a small squall line typically became involved in lightning at least 10 min before it started initiating lightning and continued to be involved at least 10 min after it ceased initiating flashes. This kind of interaction among cells makes the flash rates and spatial distribution of lightning appear more continuous than might be expected from the formation and dissipation of discrete cells. Because many storms have multiple cells, such scenarios are likely common.

We observed two 6–10-min periods of rapid substantial increases in flash rates. Both would satisfy some definitions for “lightning jumps,” which have been suggested as flags of storm intensification leading to the increased probability of severe weather (e.g., Williams et al. 1999; Schultz et al. 2009). The first and smaller of the two increases in flash rates was not related to severe weather production at all, although it was related to storm growth. The second increase in flash rates began a few minutes after the initial appearance of a signature of large, wet hail formation aloft (a TBSS and reflectivity  $>60$  dBZ) and several minutes before the hail reached the ground. However, the process driving the increase in flash rates probably was not the growth of the large, wet hail itself, and the coincidence between the peak flash rate and the hail signature reaching the ground likely was accidental.

In fact, the appearance and initial growth of the region of wet hail initially corresponded to a leveling off and a decrease in flash rates, and lightning flashes tended to avoid the region containing wet hail, probably because the charge density was smaller there (MacGorman et al. 1981; MacGorman et al. 1983; Williams 1985).

This region of lightning avoidance produced a feature like the lightning holes noted by earlier studies (Krehbiel et al. 2000; MacGorman et al. 2005; MacGorman et al. 2008) of supercell storms, but unlike previously reported cases of lightning holes, the storm analyzed here was not a supercell storm having a mesocyclone. This is the first published instance of a lightning hole involving a region of wet hail instead of a strong rotating updraft.

The flash rate increases coincided with two updraft pulses inferred from reflectivity and radial velocity observations, a relationship that is in full agreement with the findings of several studies (e.g., MacGorman et al. 1989; Ziegler and MacGorman 1994; Williams et al. 1999; Krehbiel et al. 2000; Goodman et al. 2005; Wiens et al. 2005). Both flash rate increases probably were related to the observed rapid growth of storm volume and frozen precipitation, as suggested by these studies. The second updraft pulse led to a substantially higher flash rate than the first. This higher flash rate can likely be attributed to two factors: 1) the more rapid increase in the height and volume of the storm, which increased the volume of lightning activity indicated by the LMA data, and 2) the rapid substantial growth of frozen precipitation (particularly graupel) mass and volume (inferred from the growth in the volume and magnitude of moderate-to-large reflectivities above the freezing level), which would be expected to increase electrification via field-independent interactions between graupel and ice crystals. It is also possible that the large updraft magnitudes inferred from the rapid vertical storm growth brought what was normally a lower (midlevel) charge in close proximity to the midlevel (upper) charge of opposite polarity beside the updraft, and that the increase in electric field magnitude from this closer proximity enhanced the lightning production rate. Note, too, that all theories for lightning initiation have a lower threshold of electric field magnitude at higher altitudes, so all else being equal, less charge is required to initiate lightning at higher altitudes. Thus, similar charging rates could lead to larger flash rates in taller storms.

The frequent volume scans provided by the NWRT PAR demonstrated here that using a peak in flash rates to identify the time of a relative maximum in storm intensity can be misleading in some circumstances. It is true that the initial rapid increase in flash rates was indicative of storm intensification, but flash rates subsequently increased more slowly and then decreased as the

storm's first downdraft developed and an updraft surge began simultaneously. The offsetting growth and decay within the storm probably contributed to the timing of the peak in flash rates. Another factor was the initial appearance and growth of a region in which a TBSS and reflectivity >60 dBZ indicated the growth of wet hail beginning in the second updraft surge. As discussed previously, graupel wet growth would not be expected to contribute to electrification by charge exchange during collisions with cloud ice, because the cloud ice rarely, if ever, rebounds under such conditions. The existence of a local suppression of electrification is supported by the relatively short-lived lightning hole, which was collocated with the region of wet hail in the mixed-phase region (Fig. 7). It is also likely that the number of electrically significant particles would be reduced due to increased particle coalescence in wet growth, and this would reduce the efficacy of charging processes and contribute to the lightning hole. Thus, a significant portion of mixed-phase precipitation growth probably did not contribute to the storm's electrification during the period of wet hail growth, and this likely contributed to the 2-min decrease in flash rates that followed the initial peak and preceded the second, more rapid increase in flash rates.

The above relationships suggest that lightning data provide additional information about storm intensification that could be useful to forecasters, with two cautions:

- 1) As an indication of sudden changes in the updraft mass flux through the mixed-phase region, rapidly increasing flash rates can be broadly useful in nowcasting increased potential for severe weather in the 0–20-min time frame; but in much the same way as hook echoes and mesocyclones are not direct indicators of tornadoes, lightning jumps should not be confused as an indicator of a severe weather phenomenon itself, as noted previously by Williams (2001). Schultz et al. (2009) show that a suitable algorithm for detecting lightning jumps can reveal a positive correlation with severe weather reports under at least some scenarios, even though the electrical measurements do not directly detect the severe phenomena of interest.
- 2) One must be somewhat cautious when interpreting peaks in flash rates. Although each updraft pulse in a storm contributes additional electrification, the timing of major inflections, peaks, or minima in lightning flash rates of the storm overall can depend on the competing tendencies from coevolving updrafts and downdrafts in different regions of the storm. Furthermore, one exception to the tendency for increasing electrification during precipitation growth in the

mixed-phase region appears to be the situation in which the surface of frozen precipitation becomes wet. Thus, while a large rapid increase in lightning flash rates reliably indicates the growth of a storm through and above the mixed-phase region, level or decreasing storm flash rates do not necessarily imply that updrafts or storms are in steady state or weakening.

*Acknowledgments.* Funding for this research was provided by NSF Grants ATM-0813767 and ATM-0233268. Any opinions, findings, conclusions, or recommendations expressed in this paper are those of the authors and do not necessarily reflect the views of the National Science Foundation. The authors wish to thank Drs. Ron Thomas, Bill Rison, and Paul Krehbiel for their help with data analysis, support with the required software and hardware, and assistance in general.

#### REFERENCES

- Baker, B., M. B. Baker, E. R. Jayaratne, J. Latham, and C. P. R. Saunders, 1987: The influence of diffusional growth rates on the charge transfer accompanying rebounding collisions between ice crystals and soft hailstones. *Quart. J. Roy. Meteor. Soc.*, **113**, 1193–1215.
- Biagi, C. J., K. L. Cummins, K. E. Kehoe, and E. P. Krider, 2007: National Lightning Detection Network (NLDN) performance in southern Arizona, Texas, and Oklahoma in 2003–2004. *J. Geophys. Res.*, **112**, D05208, doi:10.1029/2006JD007341.
- Black, R. A., and J. Hallett, 1999: Electrification of the hurricane. *J. Atmos. Sci.*, **56**, 2004–2028.
- Blythe, A. M., W. A. Cooper, and J. B. Jensen, 1988: A study of the source of entrained air in Montana cumuli. *J. Atmos. Sci.*, **45**, 3944–3964.
- Bringi, V. N., K. Knupp, A. Detwiler, L. Liu, I. J. Caylor, and R. A. Black, 1997: Evolution of a Florida thunderstorm during the Convection and Precipitation/Electrification Experiment: The case of 9 August 1991. *Mon. Wea. Rev.*, **125**, 2131–2160.
- Bruning, E. C., 2008: Charging regions, regions of charge, and storm structure in a partially inverted polarity supercell thunderstorm. Ph.D. dissertation, University of Oklahoma, 114 pp.
- , W. D. Rust, T. J. Schuur, D. R. MacGorman, P. R. Krehbiel, and W. Rison, 2007: Electrical and polarimetric radar observations of a multicell storm in TELEX. *Mon. Wea. Rev.*, **135**, 2525–2544.
- , —, D. R. MacGorman, M. I. Biggerstaff, and T. J. Schuur, 2010: Formation of charge structures in a supercell. *Mon. Wea. Rev.*, **138**, 3740–3761.
- Carey, L. D., and S. A. Rutledge, 1998: Electrical and multiparameter radar observations of a severe hailstorm. *J. Geophys. Res.*, **103**, 13 979–14 000.
- , and —, 2000: Relationship between precipitation and lightning in tropical island convection: A C-band polarimetric radar study. *Mon. Wea. Rev.*, **128**, 2687–2710.
- , and K. M. Buffalo, 2007: Environmental control of cloud-to-ground lightning polarity in severe storms. *Mon. Wea. Rev.*, **135**, 1327–1353.

- Changnon, S. A., 1992: Temporal and spatial relations between hail and lightning. *J. Appl. Meteor.*, **31**, 587–604.
- Coleman, L. M., T. C. Marshall, M. Stolzenburg, T. Hamlin, P. R. Krehbiel, W. Rison, and R. J. Thomas, 2003: Effects of charge and electrostatic potential on lightning propagation. *J. Geophys. Res.*, **108**, 4298, doi:10.1029/2002JD002718.
- Dash, J. G., B. L. Mason, and J. S. Wettlaufer, 2001: Theory of charge and mass transfer in ice–ice collisions. *J. Geophys. Res.*, **106**, 20 395–20 402.
- Doviak, R. J., and D. S. Zrnić, 1993: *Doppler Radar and Weather Observations*. Academic Press, 562 pp.
- Dye, J. E., J. J. Jones, A. J. Weinheimer, and W. P. Winn, 1988: Observations within two regions of charge during initial thunderstorm electrification. *Quart. J. Roy. Meteor. Soc.*, **114**, 1271–1290.
- Emersic, C., and C. P. R. Saunders, 2010: Further laboratory investigations into the relative diffusional growth rate theory of thunderstorm electrification. *Atmos. Res.*, **98**, 327–340, doi:10.1016/j.atmosres.2010.07.011.
- Foote, G. B., and H. W. Frank, 1983: Case study of a hailstorm in Colorado. Part III: Airflow from triple-Doppler measurements. *J. Atmos. Sci.*, **40**, 686–707.
- Goodman, S. J., and Coauthors, 2005: The North Alabama Lightning Mapping Array: Recent severe storm observations and future prospects. *Atmos. Res.*, **76**, 423–437.
- Heinselman, P. L., D. L. Prieznitz, K. L. Manross, T. M. Smith, and R. W. Adams, 2008: Rapid sampling of severe storms by the National Weather Radar Testbed Phased Array Radar. *Wea. Forecasting*, **23**, 808–824.
- Jacobson, E. A., and E. P. Krider, 1976: Electrostatic field changes produced by Florida lightning. *J. Atmos. Sci.*, **33**, 103–117.
- Jayarathne, E. R., and C. P. R. Saunders, 1984: The “rain-gush”, lightning, and the lower positive charge center in thunderstorms. *J. Geophys. Res.*, **89**, 11 816–11 818.
- , —, and J. Hallett, 1983: Laboratory studies of the charging of soft-hail during ice crystal interactions. *Quart. J. Roy. Meteor. Soc.*, **109**, 609–630.
- Kitagawa, N., 1992: Charge distribution of winter thunderstorms. *Res. Lett. Atmos. Electr.*, **12**, 143–153.
- , and K. Michimoto, 1994: Meteorological and electrical aspects of winter thunderclouds. *J. Geophys. Res.*, **99**, 10 713–10 721.
- Krehbiel, P. R., R. J. Thomas, W. Rison, T. Hamlin, J. Harlin, and M. Davis, 2000: GPS-based mapping system reveals lightning inside storms. *Eos, Trans. Amer. Geophys. Union*, **81**, 21–25.
- Kuhlman, K. M., C. L. Ziegler, E. R. Mansell, D. R. MacGorman, and J. M. Straka, 2006: Numerically simulated electrification and lightning of the 29 June 2000 STEPS supercell storm. *Mon. Wea. Rev.*, **134**, 2734–2757.
- , D. R. MacGorman, M. I. Biggerstaff, and P. R. Krehbiel, 2009: Lightning initiation in the anvil of supercell storms. *Geophys. Res. Lett.*, **36**, L07802, doi:10.1029/2008GL036650.
- Lang, T. J., and Coauthors, 2004: The Severe Thunderstorm Electrification and Precipitation Study. *Bull. Amer. Meteor. Soc.*, **85**, 1107–1125.
- Lund, N., D. R. MacGorman, T. J. Schuur, M. I. Biggerstaff, and W. D. Rust, 2009: Relationships between lightning location and polarimetric radar signatures in a small mesoscale convective system. *Mon. Wea. Rev.*, **137**, 4151–4170.
- MacGorman, D. R., and D. W. Burgess, 1994: Positive cloud-to-ground lightning in tornadic storms and hailstorms. *Mon. Wea. Rev.*, **122**, 1671–1697.
- , and W. D. Rust, 1998: *The Electrical Nature of Storms*. Oxford University Press, 442 pp.
- , A. A. Few, and T. L. Teer, 1981: Layered lightning activity. *J. Geophys. Res.*, **86**, 9900–9910.
- , W. L. Taylor, and A. A. Few, 1983: Lightning location from acoustic and VHF techniques relative to storm structure from 10 cm radar. *Proceedings in Atmospheric Electricity*, L. H. Ruhnke and J. Latham, Eds., A. Deepak Publishing, 377–380.
- , D. W. Burgess, V. Mazur, W. D. Rust, W. L. Taylor, and B. C. Johnson, 1989: Lightning rates relative to tornadic storm evolution on 22 May 1981. *J. Atmos. Sci.*, **46**, 221–250.
- , J. M. Straka, and C. L. Ziegler, 2001: A lightning parameterization for numerical cloud models. *J. Appl. Meteor.*, **40**, 459–478.
- , W. D. Rust, P. Krehbiel, W. Rison, E. Bruning, and K. Wiens, 2005: The electrical structure of two supercell storms during STEPS. *Mon. Wea. Rev.*, **133**, 2583–2607.
- , T. Filiaggi, R. L. Holle, and R. A. Brown, 2007: Negative cloud-to-ground lightning flash rates relative to VIL, maximum reflectivity, cell height, and cell isolation. *J. Lightning Res.*, **1**, 132–147.
- , and Coauthors, 2008: TELEX: The Thunderstorm Electrification and Lightning Experiment. *Bull. Amer. Meteor. Soc.*, **89**, 997–1013.
- Maekawa, Y., S. Fukao, Y. Sono, and F. Yoshino, 1992: Dual polarization radar observations of anomalous wintertime thunderclouds in Japan. *IEEE Trans. Geosci. Remote Sens.*, **30**, 838–844.
- Mansell, E. R., D. R. MacGorman, J. M. Straka, and C. L. Ziegler, 2002: Simulated three-dimensional branched lightning in a numerical thunderstorm model. *J. Geophys. Res.*, **107**, 4075, doi:10.1029/2000JD000244.
- , C. L. Ziegler, and E. C. Bruning, 2010: Simulated electrification of a small thunderstorm with two-moment bulk microphysics. *J. Atmos. Sci.*, **67**, 171–194.
- Marshall, T. C., and W. P. Winn, 1982: Measurements of charged precipitation in a New Mexico thunderstorm: Lower positive charge centers. *J. Geophys. Res.*, **87**, 7141–7157.
- Michimoto, K., 1991: A study of radar echoes and their relation to lightning discharge of thunderclouds in the Hokuriku district. Part I: Observation and analysis of thunderclouds in summer and winter. *J. Meteor. Soc. Japan*, **69**, 327–335.
- , 1993: A study of radar echoes and their relation to lightning discharge of thunderclouds in the Hokuriku district. Part II: Observation and analysis of “single-flash” thunderclouds in midwinter. *J. Meteor. Soc. Japan*, **71**, 195–204.
- Mitzeva, R. P., C. P. R. Saunders, and B. Tsenova, 2005: A modelling study of the effect of cloud saturation and particle growth rates on charge transfer in thunderstorm electrification. *Atmos. Res.*, **76**, 206–221.
- Pereyra, R. G., E. E. Avila, N. E. Castellano, and C. P. R. Saunders, 2000: A laboratory study of graupel charging. *J. Geophys. Res.*, **105**, 20 803–20 812.
- Riousset, J. A., V. P. Pasko, P. R. Krehbiel, R. J. Thomas, and W. Rison, 2007: Three-dimensional fractal modeling of intracloud lightning discharge in a New Mexico thunderstorm and comparison with lightning mapping observations. *J. Geophys. Res.*, **112**, D15203, doi:10.11029/12006JD007621.
- Rison, W., R. J. Thomas, P. R. Krehbiel, T. Hamlin, and J. Harlin, 1999: A GPS-based three-dimensional lightning mapping system: Initial observations in central New Mexico. *Geophys. Res. Lett.*, **26**, 3573–3576.

- Rust, W. D., and D. R. MacGorman, 2002: Possibly inverted-polarity electrical structures in thunderstorms during STEPS. *Geophys. Res. Lett.*, **29**, 1571, doi:10.1029/2001GL014303.
- , W. L. Taylor, D. R. MacGorman, and R. T. Arnold, 1981: Research on electrical properties of severe thunderstorms in the Great Plains. *Bull. Amer. Meteor. Soc.*, **62**, 1286–1293.
- , and Coauthors, 2005: Inverted-polarity electrical structures in thunderstorms in the Severe Thunderstorm Electrification and Precipitation Study (STEPS). *Atmos. Res.*, **76**, 247–271.
- Saunders, C. P. R., and I. M. Brooks, 1992: The effects of high liquid water content on thunderstorm charging. *J. Geophys. Res.*, **97**, 14 671–14 676.
- , and S. L. Peck, 1998: Laboratory studies of the influence of the rime accretion rate on charge transfer during crystal/graupel collisions. *J. Geophys. Res.*, **103**, 13 949–13 956.
- , H. Bax-Norman, E. E. Avila, and N. E. Castellano, 2004: A laboratory study of the influence of ice crystal growth conditions on subsequent charge transfer in thunderstorm electrification. *Quart. J. Roy. Meteor. Soc.*, **130**, 1395–1406.
- , —, C. Emersic, E. E. Avila, and N. E. Castellano, 2006: Laboratory studies of the effect of cloud conditions on graupel/crystal charge transfer in thunderstorm electrification. *Quart. J. Roy. Meteor. Soc.*, **132**, 2653–2673.
- Schultz, C. J., W. A. Petersen, and L. D. Carey, 2009: Preliminary development and evaluation of lightning jump algorithms for the real-time detection of severe weather. *J. Appl. Meteor. Climatol.*, **48**, 2543–2563.
- Shafer, M. A., D. R. MacGorman, and F. H. Carr, 2000: Cloud-to-ground lightning throughout the lifetime of a severe storm system in Oklahoma. *Mon. Wea. Rev.*, **128**, 1798–1716.
- Shao, X. M., and P. R. Krehbiel, 1996: The spatial and temporal development of intracloud lightning. *J. Geophys. Res.*, **101**, 26 641–26 668.
- Stith, J. L., 1992: Observations of cloud-top entrainment in cumuli. *J. Atmos. Sci.*, **49**, 1334–1347.
- Takahashi, T., 1978: Riming electrification as a charge generation mechanism in thunderstorms. *J. Atmos. Sci.*, **35**, 1536–1548.
- Taylor, W. L., E. A. Brandes, W. D. Rust, and D. R. MacGorman, 1984: Lightning activity and severe storm structure. *Geophys. Res. Lett.*, **11**, 545–548.
- Thomas, R. J., P. R. Krehbiel, W. Rison, S. J. Hunyady, W. P. Winn, T. Hamlin, and J. Harlin, 2004: Accuracy of the Lightning Mapping Array. *J. Geophys. Res.*, **109**, D14207, doi:10.1029/2004JD004549.
- Ushio, T., S. J. Heckman, H. J. Christian, and Z. I. Kawasaki, 2003: Vertical development of lightning activity observed by the LDAR system: Lightning bubbles. *J. Appl. Meteor.*, **42**, 165–174.
- Wiens, K. C., S. A. Rutledge, and S. A. Tessendorf, 2005: The 29 June 2000 supercell observed during STEPS. Part II: Lightning and charge structure. *J. Atmos. Sci.*, **62**, 4151–4177.
- Williams, E. R., 1985: Electrical discharge propagation in and around space charge clouds. *J. Geophys. Res.*, **90**, 6059–6070.
- , 2001: The electrification of severe storms. *Severe Convective Storms, Meteor. Monogr.*, No. 50, 527–561.
- , and Coauthors, 1999: The behavior of total lightning activity in severe Florida thunderstorms. *Atmos. Res.*, **51**, 245–265.
- , V. Mushtak, D. Rosenfeld, S. Goodman, and D. Boccippio, 2005: Thermodynamic conditions favorable to superlative thunderstorm updraft, mixed phase microphysics and lightning flash rate. *Atmos. Res.*, **76**, 288–306.
- Yijun, Z., P. R. Krehbiel, and L. Xinsheng, 2002: Polarity inverted intracloud discharges and electric charge structure of thunderstorm. *Chin. Sci. Bull.*, **47**, 1725–1729.
- Ziegler, C. L., and D. R. MacGorman, 1994: Observed lightning morphology relative to modeled space charge and electric field distributions in a tornadic storm. *J. Atmos. Sci.*, **51**, 833–851.
- , —, P. S. Ray, and J. E. Dye, 1991: A model evaluation of non-inductive graupel-ice charging in the early electrification of a mountain thunderstorm. *J. Geophys. Res.*, **96**, 12 833–12 855.
- Zrnić, D. S., 1987: Three-body scattering produces precipitation signature of special diagnostic-value. *Radio Sci.*, **22**, 76–86.
- , and Coauthors, 2007: Agile-beam phased array radar for weather observations. *Bull. Amer. Meteor. Soc.*, **88**, 1753–1766.